

Temperature dependent vibrational modes of glycosidic bond in disaccharide sugars

Jeong-Ah Seo, Hyun-Joung Kwon, Hyung Kook Kim and Yoon-Hwae Hwang*

Department of Nanomaterials and BK21 Nano Fusion Technology Division, Pusan National University, Miryang 627-706, Republic of Korea

Received 11 July 2007; received in revised form 4 December 2007; accepted 10 December 2007

Available online 7 January 2008

Abstract—We studied the temperature dependent vibrational modes of the glycosidic bond in trehalose, sucrose, and maltose at wavenumbers ranging from 1000 to 1200 cm^{-1} . We found that the slope of temperature dependent Raman shifts of the glycosidic bond in trehalose and sucrose changed at temperatures around 120 °C, indicating a bond length or a bond angle (dihedral and torsional angles) change. However, we did not observe any slope change in maltose because the melting temperature of maltose is very close to 120 °C. We also found, at temperatures below 120 °C, that Raman shifts of the vibrational modes of the glycosidic bond in trehalose showed the strongest temperature dependence among the three disaccharides.

© 2007 Elsevier Ltd. All rights reserved.

Keywords: Disaccharide; Raman scattering; Glycosidic bond; Trehalose; Sucrose; Maltose

1. Introduction

Sugar is a main constituent of the biological system and the systems of sugar and sugar containing materials are a matter of common interest in many research areas. The bio-protection ability of disaccharides has attracted much interest in recent years.^{1–4} The stabilizing role of disaccharides has been recognized for years in biological systems, such as proteins,^{5–11} liposomes,^{12–14} vaccines,^{15,16} enzymes,¹⁷ and membranes.^{18–21} In Nature, disaccharides seem to provide biological materials an ability to survive under extremely dry and freezing conditions. Particularly, the bio-protection ability of trehalose is superior to the other disaccharides^{22–29} and there are several possible origins of the protection ability, which include water replacement processes,^{30–32} vitrification,^{14,25} and dynamic reducers.³⁶

The bio-protection properties of disaccharides were usually interpreted on the basis of sugar–water interactions because sugars exist together with water in most the living systems. Nevertheless, we were interested in

a property of dried disaccharide because we believe that sugar by itself has an effect on the protection of biological cells through interaction with the head group of the lipid. It is a well known fact that the glycosidic linkage is the most flexible part in the structure of the disaccharides³³ and the conformation (structural rigidity and flexibility) of the glycosidic linkage is particularly important for understanding its bio-protection abilities.^{34–36}

In this paper, we studied the vibrational modes of the glycosidic bond in three disaccharides (trehalose, sucrose, and maltose) by using Raman spectroscopy. This has proved to be an effective tool for studying molecular structures and interactions.³⁷ We measured the vibrational mode of the glycosidic bond in trehalose, sucrose, and maltose at wavenumbers ranging from 1000 cm^{-1} to 1200 cm^{-1} . From the Raman measurement results, we found that the slope of the temperature dependent Raman mode of the glycosidic bond changed in trehalose and sucrose indicating a structural change in the glycosidic bond. We also found that at temperatures below 120 °C, the Raman shifts of the vibrational modes of the glycosidic bond in trehalose showed the strongest temperature dependence among the three disaccharides.

* Corresponding author. Tel.: +82 55 350 5274; fax: +82 55 353 5844; e-mail: yhwang@pusan.ac.kr

2. Experiments

We used three disaccharides: sucrose, trehalose dihydrate, and maltose monohydrate. Trehalose dihydrate was purchased from Fluka Company and all the other sugars (sucrose and maltose monohydrate) were purchased from Sigma Chemical Company. All sugars were used without further purification and the trehalose dihydrate and maltose monohydrate were dried by using a moisture analyzer (Sartorius MA100, Germany) at 100 °C for 5 h. All sugars were ground to a fine powder and pressed down into a glass vessel. To monitor any possible phase change in trehalose, we used X-ray powder diffraction technique (PANalytical X'Pert PRO, Netherlands) with Cu-K α radiation. The scan range of 2θ was from 5° to 50° at temperatures of 100 °C and 150 °C.

In Raman spectroscopy measurement, we used back-scattering geometry. The incident beam was a vertically polarized 514.5 nm green light Ar-ion laser (I90-C, Coherent, USA) at 100 mW. The scattered light was measured by using a monochromator (Acton Research, Spectra Pro-750, USA) and a charge-coupled device (Andor CCD DV420-UV, EU) at wavenumbers ranging from 1000 to 1200 cm^{-1} with a 0.5 nm ($=0.5 \times 10^{-7}$ cm) spectral resolution. The exposure time was 1 s and the spectrum was accumulated 1000 times. The temperature range used in this study was from room temperature up to the melting temperature of each disaccharide. The melting temperatures of trehalose, sucrose, and maltose were 213 °C, 185–187 °C, and 120–140 °C, respectively.

3. Results and discussion

We measured the Raman spectra of trehalose, sucrose, and maltose to observe the change in the glycosidic bond structure of the disaccharides at wavenumbers ranging from 1000 cm^{-1} to 1200 cm^{-1} with increasing temperature. The results are shown in Figures 1a–c. The Raman spectra of trehalose, sucrose, and maltose were fit by four, five, and seven Lorentzian functions, respectively. The number of Lorentzian functions was determined based on the results from the previous studies.^{38–40,43,45,46}

Figure 1a shows the Raman spectra of trehalose at temperatures ranging from 50 °C to 200 °C and each spectrum was fitted to four Lorentzian functions (T1–T4). The origins of the four peaks are the C–O stretching + C–C stretching (T1), C–O stretching + C–C stretching + COH bending (T2), C–O stretching + Ring (T3), and C–O stretching (T4) vibrational modes, respectively.^{38–40} In the Raman spectra of trehalose, we were especially interested in peaks T3 and T4 because these two peaks correspond to the vibrational modes of the glycosidic bond in the trehalose molecule. Figures 2a–d

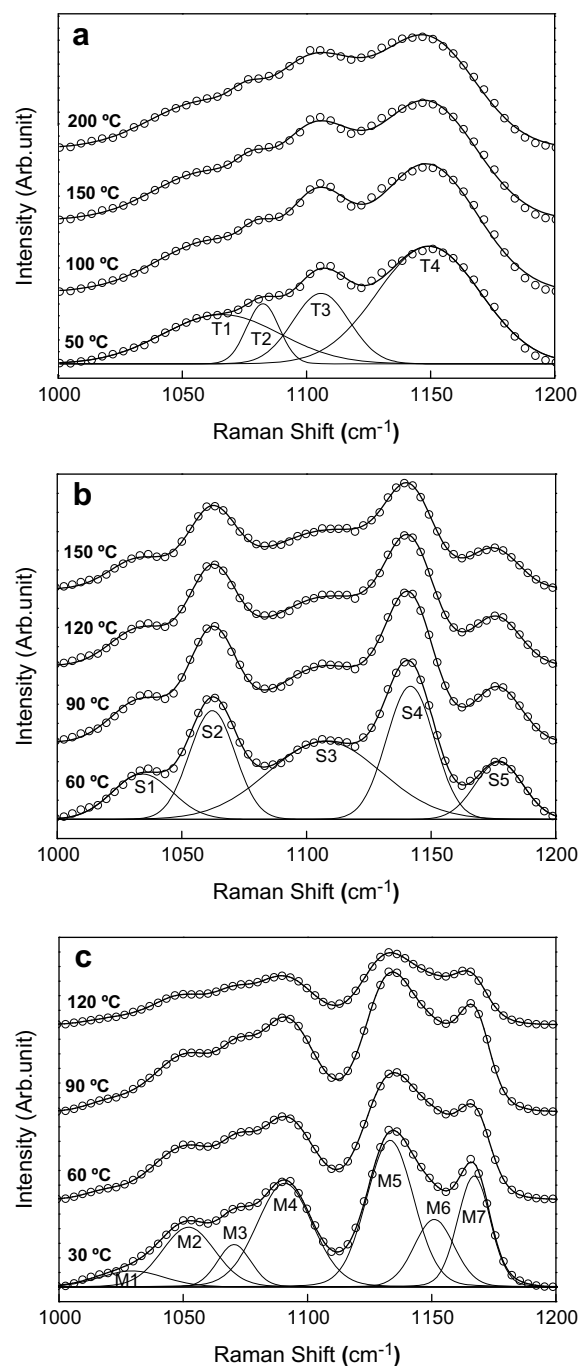


Figure 1. The temperature dependent Raman spectra of (a) trehalose, (b) sucrose, and (c) maltose in the wavenumber range of 1000–1200 cm^{-1} . The open circles are experimental results and the solid lines in fit the data to simple Lorentzian functions.

show the four temperature dependent Raman modes in trehalose at the temperatures ranging from 50 °C to 200 °C. In Figures 2a and b, the Raman shifts of peaks T1 and T2 monotonically decreased with increasing temperature. In Figures 2c and d, however, the Raman shifts of peaks T3 and T4 decreased with increasing temperature up to around 120 °C. At temperatures above

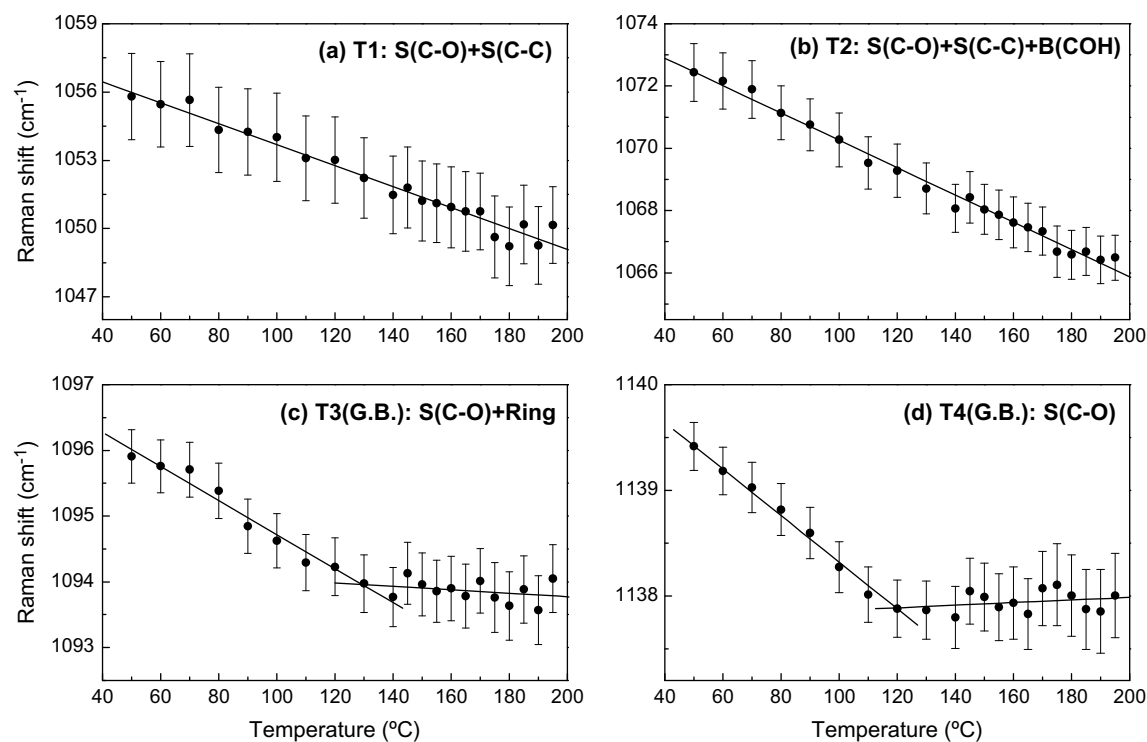


Figure 2. The temperature dependent Raman shifts in trehalose at temperatures ranging from 50 °C to 200 °C. The origins of the four peaks are (a) C–O stretching + C–C stretching (T1), (b) C–O stretching + C–C stretching + COH bending (T2), (c) C–O stretching + Ring (T3), and (d) C–O stretching (T4) vibrational modes. The solid lines in (a) and (b) are the fitted results by a linear regression.

120 °C, peaks T3 and T4 were almost temperature independent.

The temperature dependence of the glycosidic bond vibrations can be simply related to the thermal expansion of the crystal. Alers et al. found in their study that the Raman shift decreased with increasing the thermal expansion.⁵⁰ If the temperature dependence of the glycosidic bond vibration in disaccharides originated only from the thermal expansion of the crystal, there is no reason for the slope of the temperature dependent Raman shift of the glycosidic bond to change at the temperature of 120 °C. Moreover, we also found that the slope changed only in the glycosidic bond vibrations, not in the other vibrations. Therefore, we believe that the slope change of the Raman shift originates from the glycosidic bond structure change of trehalose molecule.

The slope change of vibrational spectra of disaccharides under the effect of temperature may originate from the polymorphic transformation, a crystal transformation or a hydration–dehydration phenomenon of trehalose. Trehalose undergoes a complex polymorphic transformation depending on the heating rate.⁴¹ However, as shown in Figures 3a and b, the X-ray diffraction spectra of trehalose at temperatures of 100 °C and 150 °C show the anhydrous crystalline T_β phase⁴² and did not show any differences, indicating that trehalose does not deteriorate in the temperature ranging from

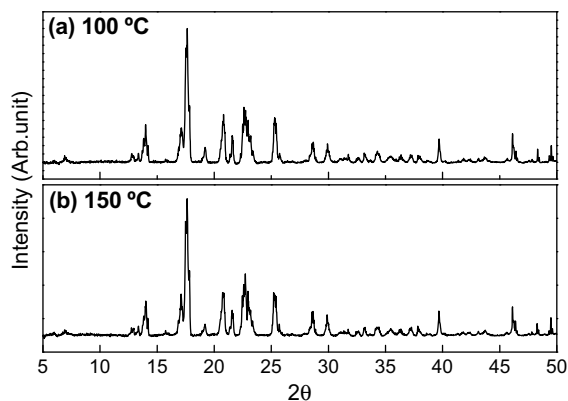


Figure 3. The X-ray diffraction spectra of trehalose at 100 °C and 150 °C.

100 °C to 150 °C. We could also exclude the possibility of the inter-molecular structure change of trehalose that could be caused by the steric hindrance and molecular associations because the XRD spectrum should convey the inter-molecular structure change. Therefore, there is no possibility that the slope change of Raman shift could originate from either a polymorphic transformation or a crystal transformation. Concerning the hydration–dehydration phenomena, we carefully checked the mass of the sample during the heating and found that the mass of trehalose does not change. Therefore, we

could conclude that the slope change of the Raman shift must have been related to the intra-molecular structure change of the trehalose molecule.

Figure 1b shows the Raman spectra of sucrose at temperatures ranging from 60 °C to 150 °C. Each spectrum was fitted to five Lorentzian functions (S1–S5) and the origins of the five peaks were the C–O stretching + C–C stretching (S1), C–O stretching + C–C stretching + Ring (S2), C–O stretching + Ring (S3), C–O stretching (S4), and CCH bending + Ring (S5) vibrational modes, respectively.^{40,43} In the case of sucrose, peaks S1 and S4 corresponded to the vibrational modes of the glycosidic bond. Figures 4a–e show the five temperature dependent Raman modes in sucrose. In Figures 4a and d, the slope of the Raman shift in peaks S1 and S4 changed at temperatures around 120 °C. This was

very similar to the temperature dependent Raman shift of the glycosidic bond of trehalose (peaks T3 and T4).

The Raman shifts of peaks S2, S3, and S5 changed monotonically with increasing temperature as shown in Figures 4b, c and e. However, as we can see in Figure 4c, the slope of Raman shifts of peak S3 is positive. The Raman shift usually decreased with increasing temperature due to a thermal expansion of material,⁵⁰ and, therefore, the increase of Raman shift in Figure 4c is an unusual process. It could be attributed to a reduction in the volume of the sucrose crystal, which, however, has never been observed. Alternatively, we may speculate that this increase of Raman shift of sucrose must be related to some molecular structure change that deserves further attention by other structural methods (diffraction and solid state NMR). The temperature dependent

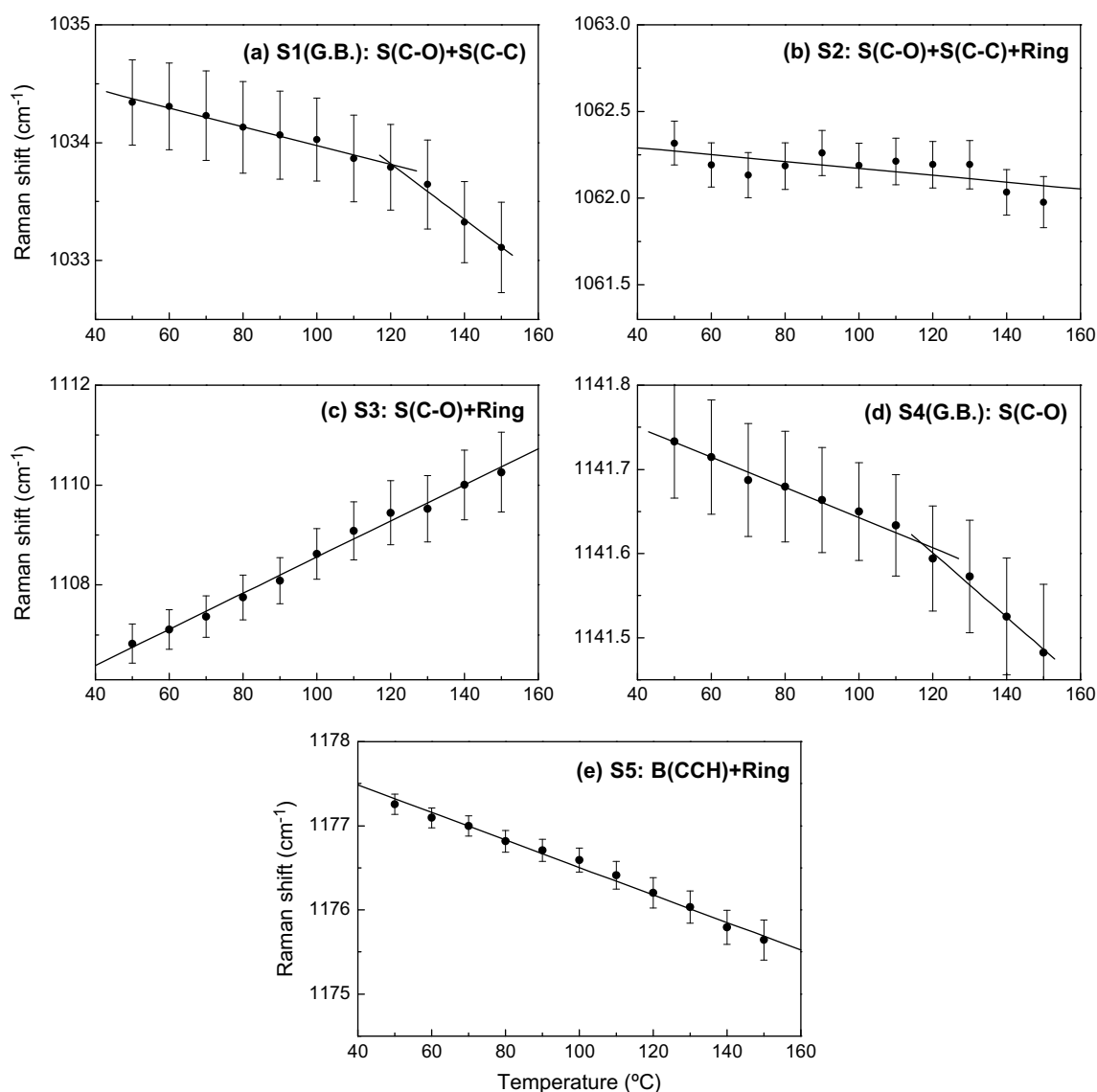


Figure 4. The temperature dependent Raman shifts in sucrose at temperatures ranging from 50 °C to 150 °C. The origins of the five peaks are the (a) C–O stretching + C–C stretching (S1), (b) C–O stretching + C–C stretching + Ring (S2), (c) C–O stretching + Ring (S3), (d) C–O stretching (S4), and (e) CCH bending + Ring (S5) vibrational modes. The solid lines in (b), (c), and (e) are the fitted results by a linear regression.

Raman shift of Figures 4a–e could be fitted by a linear regression within the error bars. However, the quality of fitting of Figures 4a and d by the linear regression is not as good as that by the fitting method used in other

data analysis. Therefore, we concluded that the slope of the temperature-dependent Raman shift of the glycosidic bond of sucrose in Figures 4a and d changed at temperatures around 120 °C.

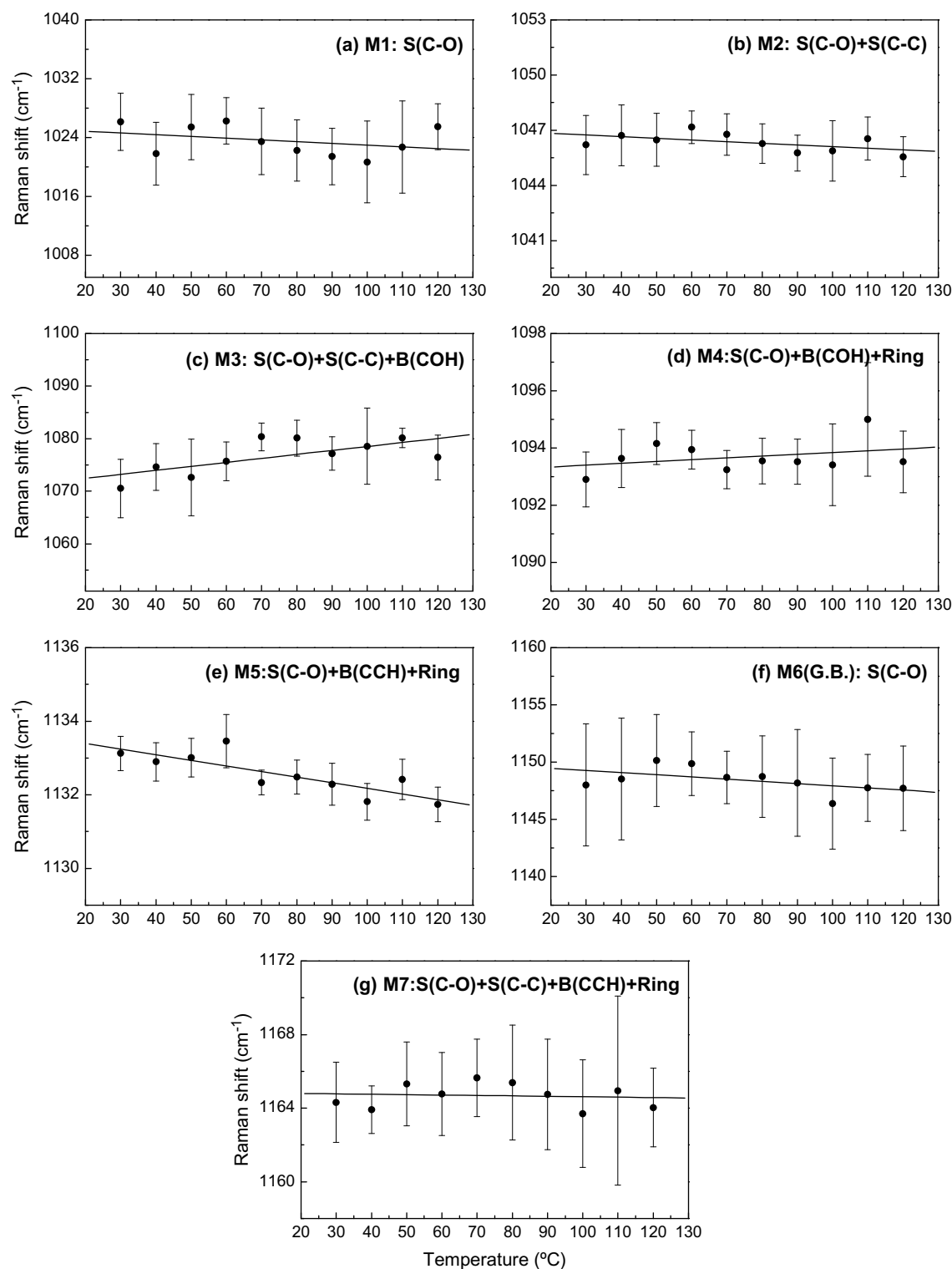


Figure 5. The temperature dependent Raman shifts in maltose at temperatures ranging from 30 °C to 120 °C. The origins of the seven peaks are the (a) C–O stretching (M1), (b) C–O stretching + C–C stretching (M2), (c) C–O stretching + C–C stretching + COH bending (M3), (d) C–O stretching + COH bending + Ring (M4), (e) C–O stretching + CCH bending + Ring (M5), (f) C–O stretching (M6), and (g) C–O stretching + C–C stretching + CCH bending + Ring (M7) vibrational modes. The solid lines are the fitted results by a linear regression.

The slope of the temperature dependent Raman shift of the glycosidic bonds in trehalose (peaks T3 and T4) and sucrose (peaks S1 and S4) changed at the same temperature of 120 °C. There are several possible causes for the change in the glycosidic bond structure, such as a broken linkage structure, a bond length change, or a bond angle change. We can disregard the broken linkage structure in this study because the temperature of 120 °C is much lower than the melting temperatures of trehalose (213 °C) and sucrose (185–187 °C). Therefore, we believe that the glycosidic bonds are fairly stable at temperatures around 120 °C.⁴⁴ We only considered bond length and angle changes as possible causes of the structural change. In the case of the bond angle change, both the dihedral angle and torsional angle changes seem to be possible.

The Raman spectra of maltose, at temperatures ranging from 30 °C to 120 °C, are shown in Figure 1c. Each Raman spectrum of maltose was fitted to seven Lorentzian functions (M1–M7) and the origins of those peaks were the C–O stretching (M1), C–O stretching + C–C stretching (M2), C–O stretching + C–C stretching + COH bending (M3), C–O stretching + COH bending + Ring (M4), C–O stretching + CCH bending + Ring (M5), C–O stretching (M6), and C–O stretching + C–C stretching + CCH bending + Ring (M7) vibrational modes, respectively.^{45,46} The Raman shifts of all seven peaks changed monotonically with increasing temperature as shown in Figures 5a–g. The peak M6 corresponds to the vibrational mode of the glycosidic bond in the maltose. As mentioned earlier, the slope of temperature dependent Raman shifts of the glycosidic bond in trehalose and sucrose changed at the same temperature of 120 °C. On the other hand, in the case of maltose, we could not observe any structural changes in the glycosidic bond in the temperature range used in this study. There is a possibility that the structure of the glycosidic bond in maltose can also be changed at temperatures around 120 °C. However, we could not measure the Raman spectra of maltose over the melting temperature because the maltose rapidly changed into a caramel at temperatures around the melting temperature (the melting temperature of maltose is known to be 120–140 °C).

We estimated the slope of the temperature dependent Raman shift, and the results are shown in Table 1. As mentioned before, the slope of the temperature dependent Raman shifts of the glycosidic bond in trehalose (peaks T3 and T4) and sucrose (peaks S1 and S4) changed at the temperature of 120 °C, but the trends of the slope changes were different. As we can see in Figures 2c and d, the Raman shifts of the glycosidic bond in trehalose were temperature independent at temperatures above 120 °C. On the other hand, as we can observe in Figures 4a and d, the temperature dependence of the Raman shifts of the glycosidic bond in sucrose became

Table 1. The slope of temperature dependent Raman shifts in trehalose, sucrose, and maltose (GB: glycosidic bond)

Trehalose (non-reducing)	T1: -0.046 ± 0.009
	T2: -0.044 ± 0.004
	T3: $-0.026 \pm 0.001 \rightarrow -0.003 \pm 0.002$ (GB)
	T4: $-0.022 \pm 0.0008 \rightarrow +0.001 \pm 0.001$ (GB)
Sucrose (non-reducing)	S1: $-0.008 \pm 0.0004 \rightarrow -0.024 \pm 0.002$ (GB)
	S2: -0.002 ± 0.001
	S3: $+0.036 \pm 0.005$
	S4: $-0.002 \pm 0.0001 \rightarrow -0.004 \pm 0.0004$ (GB)
	S5: -0.016 ± 0.001
Maltose (reducing)	M1: -0.024 ± 0.013
	M2: -0.009 ± 0.014
	M3: $+0.076 \pm 0.032$
	M4: $+0.006 \pm 0.011$
	M5: -0.015 ± 0.001
	M6: -0.019 ± 0.004 (GB)
	M7: -0.002 ± 0.001

The arrows indicate the change of slope of the temperature dependent Raman mode of GB.

stronger at temperatures above 120 °C. Therefore, the absolute value of the slope of the temperature dependent Raman shifts in trehalose decreased, but that of sucrose increased above 120 °C. At temperatures below 120 °C, the absolute value of the slope of peaks T3 and T4 in trehalose showed the highest value. This indicates that the glycosidic bond in the trehalose had the strongest temperature dependence. There are several studies connecting the flexibilities of the α,α -(1→1)-glycosidic linkage in trehalose that could be important clues in explaining its biological functions.^{34–36} In this study, we found the largest temperature dependence of the vibrational modes of the glycosidic bond in trehalose. There are several publications that already indicated a higher flexibility of glycosidic bond in trehalose with respect to maltose and sucrose.^{47–49} Our finding also indicates that the glycosidic bond of trehalose molecule was more flexible than that of sucrose and maltose. The flexibility of disaccharide could be related to the bio-protection mechanism because the higher flexibility provides better interaction between the disaccharide and the head group of the phospholipid in the biological cells.

The deviations from the expected linear negative dependence of Raman shifts with the temperature will surely deserve more work. Not only other simple reducing but also non reducing O-methylated disaccharides and cyclodextrins will have to be investigated. Furthermore, some more structural studies in the temperature range investigated here will possibly provide evidence for the hypotheses suggested by the present work.

4. Conclusion

We studied the Raman modes of trehalose, maltose, and sucrose at wavenumbers ranging from 1000 cm^{−1} to

1200 cm⁻¹. We found that the slope of the temperature dependent Raman shift of the glycosidic bond in trehalose (peaks T3 and T4) and sucrose (peaks S1 and S4) changed at temperatures around 120 °C. This indicated that the change of the glycosidic bond was possibly due to a change in bond length or bond angle (dihedral and torsional angles). However, we could not find any slope change of temperature dependent Raman shift in maltose because the melting temperature of maltose is around 120 °C. At temperatures below 120 °C, the Raman shift of vibrational modes of the glycosidic bond in trehalose showed the largest temperature dependence among the three disaccharides.

Acknowledgments

We thank H. Z. Cummins for suggesting the sugars for a glass transition study. This study was financially supported by Pusan National University in program Post-Doc. 2007. This work was also supported by the Korea Research Foundation Grants KRF-2006-521-C00060.

References

- Leslie, S. B.; Israeli, E.; Lighthart, B.; Crowe, J. H.; Crowe, L. M. *Appl. Environ. Microbiol.* **1995**, *61*, 3592–3597.
- Gouffi, K.; Pica, N.; Pichereau, V.; Blanco, C. *Appl. Environ. Microbiol.* **1999**, *65*, 1491–1500.
- Magazu, S.; Maisano, G.; Migliardo, F.; Mondelli, C. *Biophys. J.* **2004**, *86*, 3241–3249.
- Gouffi, K.; Pichereau, V.; Rolland, J. P.; Thomas, D.; Bernard, T.; Blanco, C. *J. Bacteriol.* **1998**, *180*, 5044–5051.
- Timasheff, S. N. Preferential Interactions of Water and Cosolvents with Proteins. In *Protein–Solvent Interactions*; Gregory, R., Ed.; Dekker: New York, 1995; pp 445–482.
- Miroliaei, M.; Nemat-Gorgani, M. *Enzyme Microb. Technol.* **2001**, *29*, 554–559.
- Allison, S. D.; Chang, B.; Randolph, T. W.; Carpenter, J. F. *Arch. Biochem. Biophys.* **1999**, *365*, 289–298.
- Miyawaki, O. *Biochim. Biophys. Acta Proteins Proteomics* **2007**, *1774*, 928–935.
- Ionov, R.; Hédoux, A.; Guinet, Y.; Bordat, P.; Lerbret, A.; Affouard, F.; Prevost, D.; Descamps, M. *J. Non-Cryst. Solids* **2006**, *352*, 4430–4436.
- Johnston, D. S.; Castelli, F. *Thermochim. Acta* **1989**, *144*, 195–208.
- Hannan, R. S.; Lea, C. H. *Biochim. Biophys. Acta* **1952**, *9*, 293–305.
- Christensen, D.; Foged, C.; Rosenkrands, I.; Nielsen, H. M.; Andersen, P.; Agger, E. M. *Biochim. Biophys. Acta Biomembranes* **2007**, *1768*, 2120–2129.
- Hincha, D. K.; Livingston, D. P.; Premakumar, R.; Zuther, E.; Obel, N.; Cacula, C.; Heyer, A. G. *Biochim. Biophys. Acta Biomembranes* **2007**, *1768*, 1611–1619.
- Crowe, J. H.; Leslie, S. B.; Crowe, L. M. *Cryobiology* **1994**, *31*, 355–366.
- Jonge, J. D.; Amorij, J.-P.; Hinrichs, W. L. J.; Wilschut, J.; Huckriede, A.; Frijlink, H. W. *Eur. J. Pharm. Sci.* **2007**, *32*, 33–44.
- Amorij, J.-P.; Meulenaar, J.; Hinrichs, W. L. J.; Stegmann, T.; Huckriede, A.; Coenen, F.; Frijlink, H. W. *Vaccine* **2007**, *25*, 6447–6457.
- Carpenter, J. F.; Crowe, L. M.; Crowe, J. H. *Biochim. Biophys. Acta Gen. Subjects* **1987**, *923*, 109–115.
- Crowe, J. H.; Crowe, L. M.; Chapman, D. *Science* **1984**, *223*, 701–703.
- Crowe, J.; Hoekstra, F.; Nguyen, K.; Crowe, L. *Biochim. Biophys. Acta* **1996**, *1280*, 187–196.
- Koster, K.; lei, Y.; Anderson, M.; Martin, S.; Bryant, G. *Biophys. J.* **2000**, *78*, 1932–1946.
- Ohtake, S.; Schebor, C.; Palecek, S. P.; Pablo, J. J. D. *Cryobiology* **2004**, *48*, 81–89.
- Fukuse, T.; Hirata, T.; Nakamura, T.; Ueda, M.; Kawashima, M.; Hitomi, S.; Wada, H. *Transplantation* **1999**, *68*, 110–117.
- Caffrey, M.; Fonseca, V.; Leopold, A. C. *Plant Physiol.* **1988**, *86*, 754–758.
- Crowe, J. H.; Crowe, L. M. Preservation of liposomes by freeze-drying. In *Liposome Technology*; Gregoriadis, G., Ed.; CRC Press: Boca Raton, FL, 1992.
- Crowe, J. H.; Carpenter, J. F.; Crowe, L. M. *Annu. Rev. Physiol.* **1998**, *6*, 73–103.
- Koster, K.; Webb, M. S.; Bryant, G.; Lynch, D. V. *Biochim. Biophys. Acta* **1994**, *1193*, 143–150.
- Mazzobre, M. F.; Buera, M. P.; Chirife, J. *Biotechnol. Prog.* **1997**, *13*, 195–199.
- Mazzobre, M. F.; Longinotti, M. P.; Corti, H. R.; Buera, M. P. *Cryobiology* **2001**, *43*, 199–210.
- Patist, A.; Zorb, H. *Colloids Surf., B: Biointerfaces* **2005**, *40*, 107–113.
- Bordat, P.; Lerbret, A.; Demaret, J.-P.; Affouard, F.; Descamps, M. *Europhys. Lett.* **2004**, *65*, 41–47.
- Giangiacomo, R. *Food Chem.* **2006**, *96*, 371–379.
- Lerbret, A.; Bordat, P.; Affouard, F.; Guinet, Y.; Hedoux, A.; Paccou, L.; Prevost, D.; Descamps, M. *Carbohydr. Res.* **2005**, *340*, 881–887.
- Magazù, S.; Migliardo, F.; Ramirez-Cuesta, A. J. *J. R. Soc. Interface* **2005**, *2*, 527–532.
- Dowd, M. K.; Reilly, P. J.; French, A. D. *J. Comput. Chem.* **1992**, *12*, 102–114.
- Kuttel, M. M.; Naidoo, K. J. *Carbohydr. Res.* **2005**, *340*, 875–879.
- Choi, Y.; Cho, K. W.; Jeong, K.; Jung, S. *Carbohydr. Res.* **2006**, *341*, 1020–1028.
- Mathlouthi, M.; Koenig, J. L. *Adv. Carbohydr. Chem. Biochem.* **1986**, *44*, 7–89.
- Dauchez, M.; Derreumaux, P.; Lagant, P.; Vergoten, G. *Spectrochim. Acta, Part A* **1994**, *50A*, 87–104.
- Gil, A. M.; Belton, P. S.; Felix, V. *Spectrochim. Acta, Part A* **1996**, *52*, 1649–1659.
- Kacurakova, M.; Mathlouthi, M. *Carbohydr. Res.* **1996**, *284*, 145–157.
- Sussich, F.; Urbani, R.; Princivalle, F.; Cesaro, A. *J. Am. Chem. Soc.* **1998**, *120*, 7893–7899.
- Sussich, F.; Princivalle, F.; Cesaro, A. *Carbohydr. Res.* **1999**, *322*, 113–119.
- Walther, M.; Fischer, B. M.; Jepsen, P. U. *Chem. Phys.* **2003**, *288*, 261–268.
- Fennema, O. R. *Food Chemistry*; Marcel Dekker: New York, 1985; pp 69–137.

45. Barron, L. D.; Gargaro, A. R.; Wen, Z. Q. *Carbohydr. Res.* **1991**, *210*, 39–49.
46. Dauchez, M.; Lagant, P.; Derreumaux, P.; Vergoten, G. *Spectrochim. Acta, Part A* **1994**, *50A*, 105–118.
47. Lerbret, A.; Bordat, P.; Affouard, F.; Descamps, M.; Migliardom, F. *J. Phys. Chem. B* **2005**, *109*, 11046–11057.
48. Affouard, F.; Bordat, P.; Descamps, M.; Lerbret, A.; Magazù, S.; Migliardo, F.; Ramirez-Cuesta, A. J.; Telling, M. F. T. *Chem. Phys.* **2005**, *317*, 258–266.
49. Crowe, J. H.; Crowe, L. M.; Jackson, S. A. *Arch. Biochem. Biophys.* **1983**, *220*, 477–484.
50. Alers, P.; Hintermann, H. E.; Haywardb, I. *Thin Solid Films* **1995**, *259*, 14–17.